Journal of Non - Oxide Glasses Vol. 10, No. 3, July - September 2018, p. 71 - 76

EFFECT OF Mo DOPING ON THE PHOTOVOLTAIC PROPERTIES OF Mo DOPED $Cd_{1-x}Zn_xS$ (x= 3 %) QUANTUM DOTS SYNTHESIZED BY SILAR

A. EKINCI[a], O. SAHIN[b], S. HOROZ[c,*]
[a]*Siirt University, School of Health, Department of Nursing, 56100, Siirt, Turkey*
[b]*Siirt University, Faculty of Engineering and Architecture, Department of Chemical Engineering, 56100, Siirt, Turkey*
[c]*Siirt University, Faculty of Engineering and Architecture, Department of Electrical and Electronics Engineering, 56100, Siirt, Turkey*

$Cd_{1-x}Zn_xS$ (x= 3 %) and Mo-doped $Cd_{1-x}Zn_xS$ (x= 3 %) quantum dots (QDs) with different Mo concentrations were synthesized at room temperature using successive ionic layer adsorption and reaction (SILAR) method. The aim of the study is to determine the optimum Mo concentration in Mo-doped CdZnS QDs using the incident photon to electron conversion efficiency (IPCE) measurements. To be obtained IPCE% values of samples, $Cd_{1-x}Zn_xS$ (x= 3 %) and Mo-doped $Cd_{1-x}Zn_xS$ (x= 3 %) QDs with different Mo concentrations were grown on TiO_2 coated onto FTO conductive glass substrates. As a last part of the study, the structural, elemental and optical properties of Mo-doped $Cd_{1-x}Zn_xS$ (x= 3 %) QDs containing optimum Mo content were investigated, respectively. Consequently, it appears that Mo-doped $Cd_{1-x}Zn_xS$ (x= 3 %) QDs have a higher efficiency than $Cd_{1-x}Zn_xS$ (x= 3 %) QDs and that Mo content plays an important role in this improvement.

(Received May 26, 2018; Accepted August 2, 2018)

Keywords: Characterization, Doping, Energy band gap, IPCE (%), Particle size, Synthesis

1. Introduction

Recently, the synthesis and characterization of quantum dots (QDs) of ternary alloy compounds have been extensively studied. Cadmium zinc sulfide (CdZnS) which is one of the ternary metal chalcogenide semiconductors has been the focus of scientific research because of its unusual electronic and optical properties and interesting chemical behavior [1-2]. CdZnS QDs is known to have properties in between CdS and ZnS [3]. In fact, CdZnS QDs become more attractive for solar cell production compared to CdS because they have 2.4-3.7 eV variable band gap energy [4-7]. The band gap and lattice parameters of CdZnS QDs can be altered by changing the ratio between Cd and Zn [8].

In the solar cell applications, CdS thin films have proved to be forceful. Zn addition of CdS increases both the short-circuit current and open the circuit voltage of the device, which results in a higher conversion the efficiency [9]. At the same time, the resistance of CdZnS QDs increases rapidly as the composition of zinc increases. The displacement of CdS with the higher band gap CdZnS alloys results in a reduction in window absorption losses [10]. CdZnS QDs have widely used in various optical, electronic and optoelectronic devices [11-13]. However, when CdS and ZnS QDs have been used as sensitizers in solar cells, they have some inverted properties owing to the creation of high defect density depending on its low band gap, lattice mismatch, and thickness. The theoretical and practical properties of CdS and ZnS QDs have been studied to reduce defect density by doping. The contribution efficiency mainly depends on three factors; 1) the surface morphology, (2) the shape of the nanocrystals, and (3) the surfactant in the growth solution [14-18].

* Corresponding author: sabithoroz@siirt.edu.tr

The surface morphology of ternary alloy compounds affects their optical properties. This effect is an important factor in the application of photovoltaic devices [19]. So, we have investigated the effect of Mo doping on CdZnS QDs photovoltaic properties because of the reduction of the defect densities in the alloy components of the metal doping. In this study, $Cd_{1-x}Zn_xS$ (x= 3 %) and Mo-doped $Cd_{1-x}Zn_xS$ (x= 3 %) QDs with different Mo concentrations were synthesized using successive ionic layer adsorption and reaction (SILAR) method technique at room temperature. Incident photon to electron conversion efficiency (IPCE) measurements were performed to determine the optimum Mo content in Mo-doped $Cd_{1-x}Zn_xS$ (x=3%) QDs. After the determination of the optimum Mo content in the Mo-doped $Cd_{1-x}Zn_xS$ (x=3%) QDs, the structural, elemental and optical properties of Mo-doped $Cd_{1-x}Zn_xS$ (x= 3 %) QDs containing optimum Mo content were investigated by x-ray diffraction (XRD), energy dispersive x-ray (EDX) and optical absorption measurements, respectively.

2. Materials and method

2.1 Chemicals

Cadmium acetate dehydrate (Cd $(CH_3COO)_2$. $2H_2O$), zinc acetate dehydrate (Zn $(CH_3COO).2H_2O$), sodium sulfide (Na_2S) and ammonium molybdenum tetrahydrate ($(NH_4)_6Mo_7O_{24}$) were used as the sources to synthesize $Cd_{1-x}Zn_xS$ (x= 3 %) and Mo-doped $Cd_{1-x}Zn_xS$ (x= 3 %) QDs with different Mo concentration.

2.2 Synthesis of $Cd_{1-x}Zn_xS$ (x= 3 %) QDs

To synthesize $Cd_{1-x}Zn_xS$ (x= 3 %); firstly 0.1 M Cd $(CH_3COO)_2.2\ H_2O$ and 0.003 M Zn $(CH_3COO).2H_2O$ were dissolved in a beaker containing 80 mL of ammonia, then 0.1 M Na_2S was dissolved in a second beaker containing 80 mL of ammonia.

In the typical SILAR technique, in the first step; after TiO_2 coated onto FTO conductive glass substrate was vertically immersed and kept for 1 minute in the solution containing Cd and Zn sources, it was washed with DIW and dried with N_2 gas. In the second step; the same glass substrate was vertically immersed and kept for 1 minute in the solution containing S source, it was washed with DIW and dried with N_2 gas. Thus, the first cycle was completed. The two steps mentioned above were repeated until 10 cycles were completed.

2.3 Synthesis of Mo-doped $Cd_{1-x}Zn_xS$ (x= 3 %) QDs

For preparing 0.25%, 0.5%, 1% and 3% of Mo concentration doped $Cd_{1-x}Zn_xS$ (x= 3 %) QDs, the different concentrations of $(NH_4)_6Mo_7O_{24}$ were added into solution of 1M Cd $(CH_3COO)_2$. $2H_2O$ and 0.003M Zn $(CH_3COO).2H_2O$, respectively and then followed the same procedure mentioned above.

3. Results and discussions

3.1 IPCE Analysis

The incident photon to electron conversion efficiency (IPCE) measurements were carried out to determine optimum concentration of Mo content in $Cd_{1-x}Zn_xS$ (x= 3 %) QDs. Fig. 1 indicates the IPCE spectra for Mo-doped $Cd_{1-x}Zn_xS$ (x= 3 %) QDs with different Mo concentrations at different incident light wavelengths.

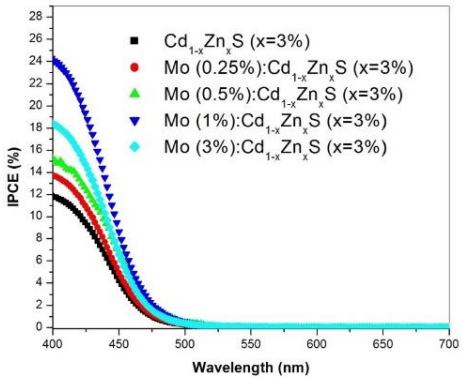

Fig. 1. The recorded IPCE spectra for Mo-doped $Cd_{1-x}Zn_xS$ (x= 3 %) QDs.

It can be clearly seen that the IIPCE (%) value at 400 nm for $Cd_{1-x}Zn_xS$ (x= 3 %) QDs shows an increment when the sample is doped with Mo content. The obtained IPCE (%) values at 400 nm for samples are given in Table 1.

Table 1. The obtained IPCE (%) value for Mo-doped $Cd_{1-x}Zn_xS$ (x= 3 %) QDs.

Samples (QDs)	IPCE (%) values at 400 nm
$Cd_{1-x}Zn_xS$ (x= 3 %)	11.82
Mo (0.25%): $Cd_{1-x}Zn_xS$ (x= 3 %)	13.68
Mo (0.5%): $Cd_{1-x}Zn_xS$ (x= 3 %)	15.02
Mo (1%): $Cd_{1-x}Zn_xS$ (x= 3 %)	24.01
Mo (3%): $Cd_{1-x}Zn_xS$ (x= 3 %)	18.22

There are two important observations should be noted that (1) the IPCE (%) efficiency is increased with the Mo doping, which suggests the QD solar cell efficiency can be enhanced by Mo doping due to widened absorption windows. (2) It can be clearly seen from the Table 1, the optimum Mo concentration in Mo-doped $Cd_{1-x}Zn_xS$ (x= 3 %) QDs was determined as 1%. The other steps of our study are to investigate structural, elemental and optical properties of Mo (1%): $Cd_{1-x}Zn_xS$ (x=3%) that they have the highest IPCE value in their category.

3.2 XRD analysis

Fig. 1 (a-b) illustrates the XRD spectra for $Cd_{1-x}Zn_xS$ (x=3%) and Mo (1%): $Cd_{1-x}Zn_xS$ (x=3%), respectively. The observed broad diffraction patterns are related to (111), (220) and (311) planes. It is an indication that the recorded patterns for both samples can be indexed as the zinc blende (cubic) phase structure of CdS, which are consistent with the standard card (JCPD No: 65-2887). No impurity peak was observed, showing that Mo ions could substitute Cd ion without any change in the structure. The particle size of QDs can be calculated using the recorded XRD patterns. Thus, the effect Mo dopant on the particle size of $Cd_{1-x}Zn_xS$ (x=3%) QDs may be investigated. It is well known that Debye-Scherrer relation given in Equation 1 was used to calculate the particle size.

$$d = 0.9\,\lambda / (\beta \cos\theta) \quad (1)$$

Where d is the mean size of the QDs, λ is the wavelength of x-ray, β is the broadening measured as FWHM in radians, and θ is Bragg's diffraction angle. The particle size of Mo (1%): $Cd_{1-x}Zn_xS$ (x=3%) QDs was calculated as 2.59 nm while this value for $Cd_{1-x}Zn_xS$ (x=3%) QDs was 2.63 nm. As can be seen the results obtained, Mo doping has an active role in changing the particle size of

$Cd_{1-x}Zn_xS$ (x=3%) QDs. The Mo ions occupy the regular lattice site of Cd ions that what may be possible reason for the decrease in the particle size.

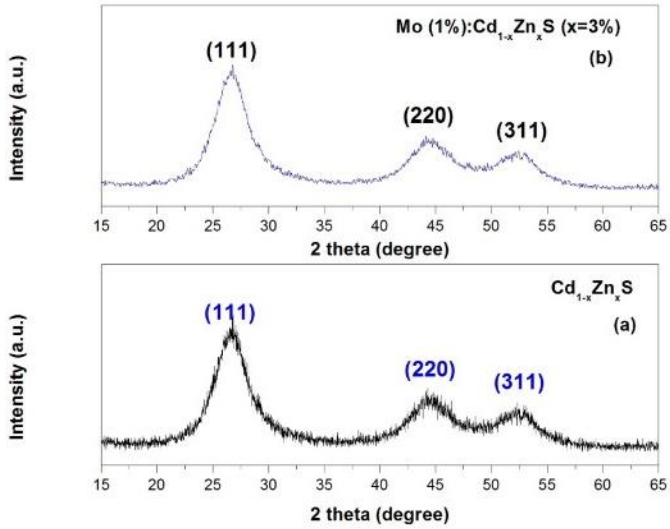

Fig. 2. The recorded XRD patterns for (a) $Cd_{1-x}Zn_xS$ (x=3%) and (b) Mo (1%): $Cd_{1-x}Zn_xS$ (x=3%) QDs.

3.3 Optical absorption analysis

The energy band gap of $Cd_{1-x}Zn_xS$ (x=3%) and Mo (1%): $Cd_{1-x}Zn_xS$ (x=3%) was analyzed by UV-visible absorption spectroscopy. It is well known that the band gap of semiconductor QDs can be altered by doping. The recorded optical absorption spectra for both samples are demonstrated in Fig. 3.

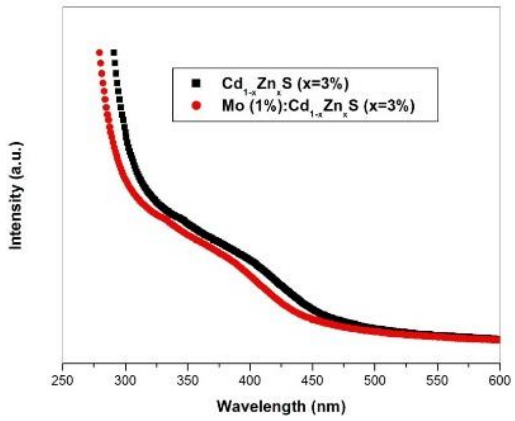

Fig. 3. The recorded UV-VIS absorption spectrums for $Cd_{1-x}Zn_xS$ (x=3%) and Mo (1%): $Cd_{1-x}Zn_xS$ (x=3%).

It can be clearly seen that the band edge of Mo (1%): $Cd_{1-x}Zn_xS$ (x=3%) QDs shifts to shorter wavelength compare compared with $Cd_{1-x}Zn_xS$ (x=3%) QDs. The reason of this shift (called blue-shift) could be that Mo ions, which result in the crystal size to decrease, reside instead of Cd ions. This also confirms the existence of quantum confinement effect on Mo (1%): $Cd_{1-x}Zn_xS$ (x=3%) in the presence of Mo dopant.

To calculate the band gap energy for both samples, Tauc relation, referred to in Equation 2, were used.

$$\alpha h\upsilon = C(h\upsilon - Eg)^n \quad (2)$$

Where α is the absorption coefficient, n=1/2 or 2 for direct or indirect allowed transition, respectively, C is the characteristic parameter for respective transitions, hυ is photon energy and Eg is energy band gap. Fig. 4 demonstrates $(\alpha h\upsilon)^2$ versus hυ for $Cd_{1-x}Zn_xS$ (x=3%) and Mo (1%): $Cd_{1-x}Zn_xS$ (x=3%).

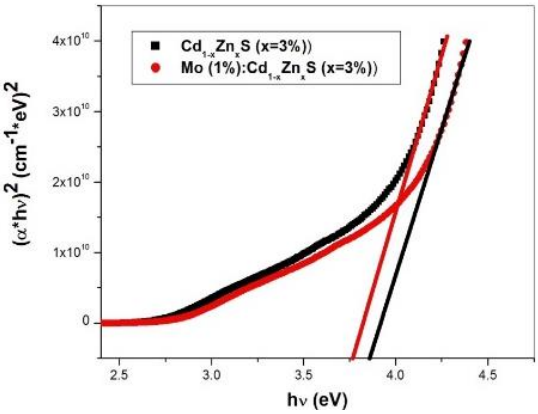

Fig. 4. $(\alpha h\upsilon)^2$ vs hυ curves for $Cd_{1-x}Zn_xS$ (x=3%) and Mo (1%): $Cd_{1-x}Zn_xS$ (x=3%).

The band gap value of $Cd_{1-x}Zn_xS$ (x=3%) and Mo (1%): $Cd_{1-x}Zn_xS$ (x=3%) was determined as 3.76 and 3.87 eV, respectively. Hence, it can be said that Mo content results in the reduction in size of $Cd_{1-x}Zn_xS$ (x=3%) (See particle size obtained from the XRD) increases the band gap of $Cd_{1-x}Zn_xS$ (x=3%).

3.4 EDX analysis

The energy dispersive x-ray (EDX) spectrum was used to confirm the elemental compositions of $Cd_{1-x}Zn_xS$ (x=3%) and Mo (1%): $Cd_{1-x}Zn_xS$ (x=3%). The peaks obtained from the EDX spectrums for $Cd_{1-x}Zn_xS$ (x=3%) and Mo (1%): $Cd_{1-x}Zn_xS$ (x=3%) are shown in Figure 5(a-b), respectively, are associated with Cd, Zn, S and Mo. The obtained EDX spectra shown in Figure 5b proves that Mo content is successfully doped into $Cd_{1-x}Zn_xS$ (x=3%).

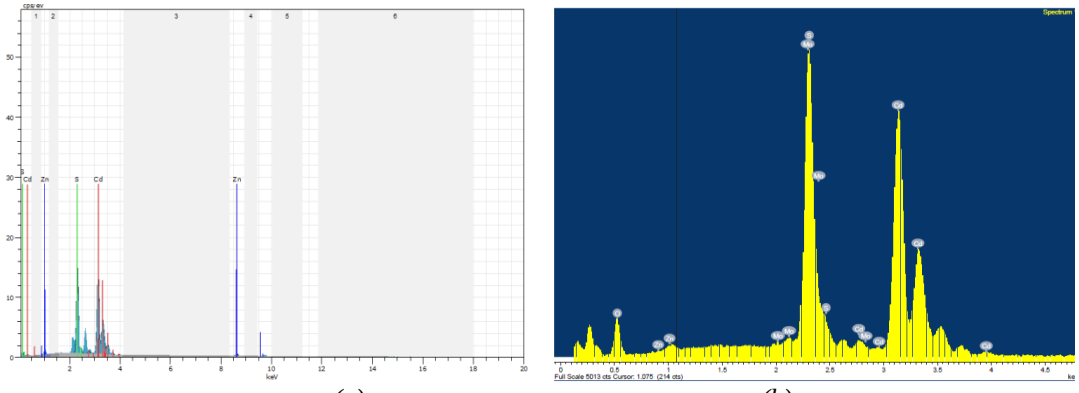

(a) *(b)*

Fig. 5. (a) The recorded EXD spectrums for $Cd_{1-x}Zn_xS$ (x=3%); (b) The recorded EXD spectrums for Mo (1%): $Cd_{1-x}Zn_xS$ (x=3%).

The elemental percentages for both samples obtained from EDX patterns are given in Table 2.

Table 2. The elemental percentages for $Cd_{1-x}Zn_xS$ (x=3%) and Mo (1%): $Cd_{1-x}Zn_xS$ (x=3%).

Elements	Elemental percentages for $Cd_{1-x}Zn_xS$ (x=3%)	Elemental percentages for Mo (1%): $Cd_{1-x}Zn_xS$ (x=3%)
Cd	47.27	48.13
Zn	1.61	1.72
S	51.12	49.38
Mo	-	0.77

4. Conclusions

The SILAR method at room temperature was used to synthesize $Cd_{1-x}Zn_xS$ (x= 3 %) and Mo-doped $Cd_{1-x}Zn_xS$ (x= 3 %) QDs with different Mo concentration. IPCE measurements were carried out to determine the optimum Mo concentration in $Cd_{1-x}Zn_xS$ (x= 3 %) QDs with different Mo concentration. The obtained IPCE results indicate that (1) Mo dopant plays an important role to enhance the efficiency of CdZnS based solar cells (2) Mo (1%): $Cd_{1-x}Zn_xS$ (x=3%) has the highest IPCE (%) value compared with other Mo concentrations.

In the second part of current study, particle size and energy band gap of $Cd_{1-x}Zn_xS$ (x= 3 %) and Mo (1%): $Cd_{1-x}Zn_xS$ (x=3%) were compared. It was found that the particle size of Mo (1%): $Cd_{1-x}Zn_xS$ (x=3%) QDs is calculated as 2.59 nm while this value for $Cd_{1-x}Zn_xS$ (x=3%) QDs is 2.63 nm. The band gap value of $Cd_{1-x}Zn_xS$ (x=3%) and Mo (1%): $Cd_{1-x}Zn_xS$ (x=3%) was determined as 3.76 and 3.87 eV, respectively. Hence, it can be said that Mo content results in the reduction in size of $Cd_{1-x}Zn_xS$ (x=3%) (See particle size obtained from the XRD) increases the band gap of $Cd_{1-x}Zn_xS$ (x=3%).

Consequently, our result suggests particle size, energy band gap and IPCE (%) values of $Cd_{1-x}Zn_xS$ (x=3%) can be altered by Mo content.

References

[1] S. Sain, S. Patra, S. K. Pradhan, Materials Research Bulletin **47**, 1062 (2012).
[2] L. E. Brus, Appl. Phys. A **53**, 465 (1991).
[3] L. P. Deshmukh et al., Indian J. Pure Appl. Phys. **35**, 428 (1997).
[4] A. P. Alivisatos, J. Phys. Chem. **100**, 13226 (1996).
[5] L. Brus, IEEE J. Quantum Electron. QE-229 (1986) 1909–1914.
[6] M. Maqbool, I. Ahmad, H. H. Richardson, M. E. Kordesch, Appl. Phys. Lett. **91**, (2007) 511
[7] R. S. Feigelson, A. N. Diage, S. Y. Yin et al., J. Appl. Phys. **48,** 3162 (1977).
[8] T. P. Kumara, S. S. kumara, K. Sankaranarayanan, Applied Surface Science **257**, 1923 (2011).
[9] D. Patıdar, N. S. Saxena, T. P. Sharma, Journal of Modern Optics **55**, 79 (2008).
[10] T. Gruszecki, B. Holmstrom, Sol. Ener. Mater. Sol. Cells **31**, 227 (1993).
[11] J. H. Lee, W. C. Song, K. J. Yang, Y. S. Yoo, Thin Solid Films **416**, 184 (2002).
[12] T. Yamaguchi, J. Matsufusa, A. Yoshida, Jpn. J. Appl. Phys. **3**, 703 (1992).
[13] X. Wu, Sol. Energy **77**, 803 (2004).
[14] S. Y. Kim, D. S. Kim, B. T. Ahn, H. B. Im, J. Mater. Sci. Mater. Electron. **4**, 178 (1993).
[15] B. J. Wu, H. Cheng, S. Guha, M. A. Hasse, J. M. De Puydt, G. Meis-Haugen, J. Qiu, Appl. Phys. Lett. **63**, 2935 (1993).
[16] G. Sharma, P. Chawl, S. P. Locha, N. Singh, Radiat. Effects Defects Solids **164**, 763 (2009).
[17] T. Yamaguchi, Y. Yamamoto, T. Tanaka, A. Yoshida Thin Solid Films **343**, 51 (1996).
[18] L. Saravanan, A. Pandurangan, R. Jayavel, Mater. Lett. **66**, 343 (2012).
[19] M. Green, Z. Hussain, J. Appl. Phys. **69**, 7788 (1991).